Article

Mechanism of Intramolecular Electron Transfer in the Photoexcited Zn-Substituted Cytochrome *c*: Theoretical and Experimental Perspective

Yuichi Tokita, Jusuke Shimura, Hiroshi Nakajima, Yoshio Goto, and Yoshihito Watanabe

J. Am. Chem. Soc., **2008**, 130 (15), 5302-5310 • DOI: 10.1021/ja711324t • Publication Date (Web): 19 March 2008

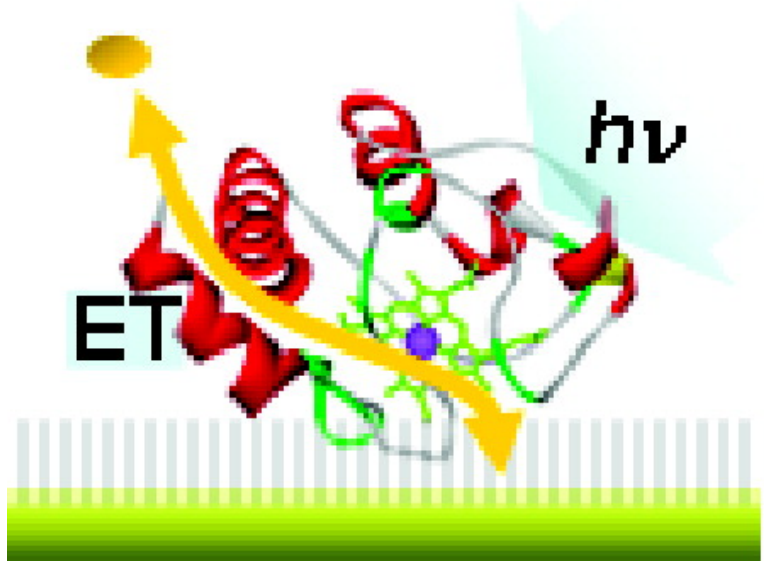

J|A|C|S
ARTICLES

Published on Web 03/19/2008

Mechanism of Intramolecular Electron Transfer in the Photoexcited Zn-Substituted Cytochrome *c*: Theoretical and Experimental Perspective

Yuichi Tokita,*,† Jusuke Shimura,† Hiroshi Nakajima,‡ Yoshio Goto,† and Yoshihito Watanabe*,§

Materials Laboratories, Sony Corporation, 4-16-1 Okata, Atsugi, Kanagawa 243-0021, Japan, Department of Chemistry, Graduate School of Science, Nagoya University, Furo-cho, Chikusa-ku, Nagoya 464-8602, Japan, and Research Center for Materials Science, Nagoya University, Furo-cho, Chikusa-ku, Nagoya 464-8602, Japan

Received December 21, 2007; E-mail: yuichi.tokita@jp.sony.com

Abstract: Photoinduced electron transfer (ET) in zinc-substituted cytochrome *c* (Zn-cyt *c*) has been utilized in many studies on the long-range ET in protein. Attempting to understand its ET mechanism in terms of electronic structure of the molecule, we have calculated an all-electron wave function for the ground-state of Zn-cyt *c* on the basis of density functional theory (DFT). The four molecular orbitals (MOs) responsible for excitation by UV–vis light (Gouterman's 4-orbitals) are assigned on the basis of the excited states of chromophore model for Zn−porphine complex calculated with the time-dependent DFT method. ET rates between each Gouterman's 4-orbitals and other MOs were estimated using Fermi's golden rule. It appeared that the two occupied MOs of the 4-orbitals show exclusively higher ET rate from/to particular MOs that localize on outermost amino acid residues (Lys 7 or Asn 54), respectively, whereas ET rates involving the two unoccupied MOs of the 4-orbitals are much slower. These results imply that the intramolecular ET in photoexcited Zn-cyt *c* is governed by the hole transfer through occupied MOs. The couplings of MOs between zinc porphyrin core and specific amino acid residues on the protein surface have been demonstrated in Zn-cyt *c* immobilized on an Au electrode via carboxylic acid group-terminated self-assembled monolayer. The Zn-cyt *c*-modified electrode showed photocurrents responsible for photoillumination. The action spectrum of the photocurrent was identical with the absorption spectrum of Zn-cyt *c*, indicating photoinduced electron conduction *via occupied MOs*. The voltage dependence of the photocurrent appeared to be linear and bidirectional like a photoconductor, which strongly supports the intramolecular ET mechanism in Zn-cyt *c* proposed on the basis of the theoretical calculations.

Introduction

Electron transfer (ET) plays important roles in chemistry, biology, and physics. Especially, the intramolecular ET in protein has been investigated in detail by many groups to elucidate the factors that control the rate of these nonadiabatic reactions.[1–8] The most remarkable aspect of ET in protein is that it occurs via quantum mechanical tunneling. Typically, redox centers in protein that exchange an electron are separated at the distance of 1.5–3.0 nm, though electron tunneling over such long distances would be impossible in vacuum. For example, in the bacterial reaction center, an excited electron on the bacteriochlorophyll dimer migrates to the bacteriopheophytin (1.7 nm) in a high efficiency to carry out energy conversion of light.[8–11] In the long-range ET in protein, the rate constant (k) is found to be proportional to a donor–acceptor electronic coupling strength which is the square of an electronic tunneling matrix element (T_{DA}) and to a nuclear Franck–Condon factor (FC):[12–14]

$$k = \frac{2\pi}{\hbar}|T_{DA}|^2(\mathrm{FC}) \quad (1)$$

† Sony Corporation.
‡ Graduate School of Science, Nagoya University.
§ Research Center for Materials Science, Nagoya University.

(1) Balzani, V. *Electron Transfer in Chemistry*; Wiley-VCH: Weinheim, Germany, 2001; Vol. 3.
(2) Willner, I.; Katz, E. *Bioelectronics*; Wiley-VCH: Weinheim, Germany, 2005.
(3) Bertini, I.; Gray, H. B.; Lippard, S. J.; Valentine, J. S. *Bioinorganic Chemistry*; University Science Books: Mill Valley, CA, 1994; p 315–363.
(4) Wuttke, D. S.; Bjerrum, M. J.; Winkler, J. R.; Gray, H. B. *Science* **1992**, *256*, 1007–1009.
(5) Langen, R.; Chang, I. J.; Germanas, J. P.; Richards, J. H.; Winkler, J. R.; Gray, H. B. *Science* **1995**, *268*, 1733–1735.
(6) Page, C. C.; Moser, C. C.; Chen, X. X.; Dutton, P. L. *Nature* **1999**, *402*, 47–52.
(7) Moser, C. C.; Keske, J. M.; Warncke, K.; Farid, R. S.; Dutton, P. L. *Nature* **1992**, *355*, 796–802.
(8) Deisenhofer, J.; Epp, O.; Miki, K.; Huber, R.; Michel, H. *J. Mol. Biol.* **1984**, *180*, 385–98.
(9) Deisenhofer, J.; Michel, H. *Science* **1989**, *245*, 1463–1473.
(10) Michel, H.; Weyer, K. A.; Gruenberg, H.; Dunger, I.; Oesterhelt, D.; Lottspeich, F. *EMBO J.* **1986**, *5*, 1149–58.
(11) Plato, M.; Mobius, K.; Michel-Beyerle, M. E.; Bixon, M.; Jortner, J. *J. Am. Chem. Soc.* **1988**, *110*, 7279–7285.
(12) Marcus, R. A. *J. Chem. Phys.* **1956**, *24*, 979–989.
(13) Levich, V. G. *Adv. Electrochem. Eng.* **1965**, *4*, 429.
(14) Jortner, J. *J. Am. Chem. Soc.* **1980**, *102*, 6676–6686.

 10.1021/ja711324t CCC: $40.75

In recent decades, many theoretical researchers have devoted efforts to clarify the T_{DA} term.[1,2,15–24] However, because of the computational and theoretical limits in performing a first principle quantum chemical calculation of a whole structure of protein, T_{DA} was described in some approximated models such as the one-electron and/or the tight binding schemes, etc.[15] Therefore, theoretical studies have not yet provided answers to the essential issues of ET in protein, that is, the pathway problem and the tunneling mechanism.

Under these circumstances, the long-range ET in protein has been experimentally studied by several groups. Dutton and coworkers proposed the distance-determined ET rate model on the basis of what they observed in multiredox center oxidoreductase systems,[6,7] while Gray and colleagues ruthenized the surface of cytchrome *c* and examined its photoinduced ET from ruthenium complex to heme. They prepared series of surface-modified mutants and found that the ET rate is not simply dependent upon the distance between donor and acceptor moiety. Rather, it appeared that the rate is correlated to the number of bonds connecting donor and acceptor or to the secondary structure in the protein.[3–5] The manner of ET through peptide insulator in a protein could be answered if the precise electronic states were determined, and at the same time, the two models may be consistently explained.

Recently, a DFT-based program to perform whole–electron calculation of proteins called Protein DF was developed by Kashiwagi and colleagues.[25] The program processes calculation of fragment peptides of a protein, with which larger fragments of the protein are built up to calculate the final, whole structure of the protein. By using this method, Sato et al. have succeeded in characterizing horse heart cytochrome *c*[26] and insulin hexamer.[27]

In this paper, we computed the all-electron wave function of Zn-substituted cytochrome *c* (Zn-cyt *c*) by using Protein DF. We chose Zn-cyt *c* because the intramolecular ET reaction in photoexcited Zn-cyt *c* has been well-investigated and the detailed structural information is available.[28–37] For the excited states, we performed a time-dependent DFT (TDDFT) calculation of the chromophore model (CM) consisting of Zn-porphine with the two axial ligands and we have assigned molecular orbitals (MOs) responsible for the excited states of Zn-cyt *c*.[38]

To investigate the mechanism of photoexcited ET in Zn-cyt *c*, we applied Fermi's golden rule[39,40] to the obtained MOs, and estimated the ET rate from Gouterman's 4-orbitals to all the other MOs each by each.[38] Surprisingly, the two occupied orbitals are strongly coupled with specific MOs localized on outermost amino acid residues, respectively: asparagine-54 (Asn54) or lysine-7 (Lys7). The Fermi's golden rule-based analyses suggest that the long distance ET in photoexcited Zn-cyt *c* is originated by a hole-transfer (HT) through the occupied MOs. This mechanism was supported by the observation of ohmic behavior of photocurrents generated by Zn-cyt *c* immobilized on a gold electrode.

Experimental Section

Computation. The horse heart Zn-cyt *c* contains 104 amino acid residues and one *c*-type Zn-protoporphyrin. The protoporphyrin is bound covalently to polypeptide (apoprotein) of Zn-cyt *c* via thioether bonds between two vinyl side chains and Cys14 and Cys17. Residues His18 and Met80 form the fifth and sixth axial ligands of zinc-protoporphyrin, respectively. The numbers of atoms and electrons are 1764 and 6590, respectively.

The coordinate of Zn-cyt *c* (horse heart) was obtained from the protein data bank as 1m60.[41] A molecular mechanics calculation was performed using the generalized Born method (dielectric constant is 80) with Discovery Studio Modeling 1.5 (force field: CHARMm) to relax local structure distortions, in the state that the structure of Zn-protoporphyrin was fixed.[42,43] At the neutralization, Na^+ and Cl^- ions were placed around the anionic and cationic residues, respectively. For an anionic residue where a Na^+ ion could not be placed for steric reason, a hydrogen atom was added to the carbonyl oxygen with 0.96 Å fixed bond length in the direction of the nearest hydrogen of water molecule. Whereas for a cationic residue where Cl^- ion could not be placed for steric reason, the hydrogen nearest to an oxygen of water molecules was removed.[26] A total of 5258 water molecules (TIP3) were placed around the protein. To relax the Na^+ and Cl^- ions, all water molecules and Na^+ and Cl^- ions were subjected to a molecular mechanics energy minimum calculation under a fixed coordinate of the protein structure. In the DFT calculation, the TIP3 water molecules were removed and Na^+ and Cl^- ions were treated as point charges $+1$ and -1, respectively.

The all-electron calculation of Zn-cyt *c* was carried out by using the Gaussian-based DFT[44] program, proteinDF[25] with VWN functional[45,46] and sg-1 grid,[47] following the method for native

(15) Newton, M. D. *Chem. Rev.* **1991**, *91*, 767–792.
(16) Stuchebrukhov, A. A. *Theor. Chem. Acc.* **2003**, *110*, 291–306.
(17) Regan, J. J.; Risser, S. M.; Beratan, D. N.; Onuchic, J. N. *J. Phys. Chem.* **1993**, *97*, 13083–13088.
(18) Siddarth, P.; Marcus, R. A. *J. Phys. Chem.* **1993**, *97*, 13078–13082.
(19) Wolfgang, J.; Risser, S. M.; Priyadarshy, S.; Beratan, D. N. *J. Phys. Chem. B* **1997**, *101*, 2986–2991.
(20) Skourtis, S. S.; Balabin, I. A.; Kawatsu, T.; Beratan, D. N. *Proc. Natl. Acad. Sci. U.S.A.* **2005**, *102*, 3552–7.
(21) Nakatsuji, H.; Hasegawa, J.; Ohkawa, K. *Chem. Phys. Lett.* **1998**, *296*, 499–504.
(22) Hasegawa, J.; Nakatsuji, H. *J. Phys. Chem. B* **1998**, *102*, 10420–10430.
(23) Hasegawa, J. Y.; Nakatsuji, H. *Chem. Lett.* **2005**, *34*, 1242–1243.
(24) Beratan, D. N.; Onuchic, J. N.; Winkler, J. R.; Gray, H. B. *Science* **1992**, *258*, 1740–1741.
(25) Sato, F.; Shigemitsu, Y.; Okazaki, I.; Yahiro, S.; Fukue, M.; Kozuru, S.; Kashiwagi, H. *Int. J. Quantum Chem.* **1997**, *63*, 245–256.
(26) Sato, F.; Yoshihiro, T.; Era, M.; Kashiwagi, H. *Chem. Phys. Lett.* **2001**, *341*, 645–651.
(27) Inaba, T.; Tahara, S.; Nisikawa, N.; Kashiwagi, H.; Sato, F. *J. Comput. Chem.* **2005**, *26*, 987–993.
(28) Lampa-Pastirk, S.; Beck, W. F. *J. Phys. Chem. B* **2004**, *108*, 16288–16294.
(29) Lampa-Pastirk, S.; Lafuente, R. C.; Beck, W. F. *J. Phys. Chem. B* **2004**, *108*, 12602–12607.
(30) Kim, J. E.; Pribisko, M. A.; Gray, H. B.; Winkler, J. R. *Inorg. Chem.* **2004**, *43*, 7953–7960.
(31) Lee, J. C.; Chang, I. J.; Gray, H. B.; Winkler, J. R. *J. Mol. Biol.* **2002**, *320*, 159–164.
(32) Chang, I. J.; Lee, J. C.; Winkler, J. R.; Gray, H. B. *Proc. Natl. Acad. Sci. U.S.A.* **2003**, *100*, 3838–3840.
(33) Zhou, J. S.; Kostic, N. M. *J. Am. Chem. Soc.* **1993**, *115*, 10796–10804.
(34) Furukawa, Y.; Ishimori, K.; Morishima, I. *Biochemistry* **2002**, *41*, 9824–9832.
(35) Zhou, J. S.; Tran, S. T.; McLendon, G.; Hoffman, B. M. *J. Am. Chem. Soc.* **1997**, *119*, 269–277.
(36) Elias, H.; Chou, M. H.; Winkler, J. R. *J. Am. Chem. Soc.* **1988**, *110*, 429–434.
(37) Braun, M.; Atalick, S.; Guldi, D. M.; Lanig, H.; Brettreich, M.; Burghardt, S.; Hatzimarinaki, M.; Ravanelli, E.; Prato, M.; van Eldik, R.; Hirsch, A. *Chem.-Eur. J.* **2003**, *9*, 3867–3875.
(38) Dolphin, D. *The Porphyrins*; Academic Press: New York, 1977.
(39) Dirac, P. A. M. *Proc. R. Soc. London, A* **1927**, *114*, 243–265.
(40) Fermi, E. *Nuclear Physics*; University of Chicago Press: Chicago, IL, 1950.
(41) Qian, C.; Yao, Y.; Tong, Y.; Wang, J.; Tang, W. *J. Biol. Inorg. Chem.* **2003**, *8*, 394–400.
(42) Cramer, C. J.; Truhlar, D. G. *Chem. Rev.* **1999**, *99*, 2161–2200.
(43) *Discovery Studio*, version 1.5; Accelrys Inc.: San Diego, CA, 2006.
(44) Andzelm, J.; Wimmer, E. *J. Chem. Phys.* **1992**, *96*, 1280–1303.
(45) Vosko, S.; Wilk, L.; Nusair, M. *Can. J. Phys.* **1980**, *58*, 1200–1211.
(46) Slater, J. C. *Quantum Theory of Molecular and Solids*; McGraw-Hill: New York, 1974; Vol. 4.

Table 1. Basis and Auxiliary Function Sets for Computation

atom	CGTO[a] Set for MO	Auxiliary function set for electron density and XC potentials[e]
Zn	(63321/5211/41)[b]	10s5p5d
S	(6321/521/1)[c]	9s4p4d
N,C,O	(621/41)[d]	7s2p
H	(41)[c]	4s1p

[a] Contracted Gaussian-type orbital. [b] DZVP2 level basis.[48] [c] DZVP level basis.[48] [d] DZV level basis.[49] [e] Reference 26.

cytochrome *c* reported by Sato et al.[26] The basis and auxiliary function sets used are listed in Table 1.[48,49] The effective initial guess was constructed using quasi-canonical localized orbitals (QCLOs).[50] First, we decomposed Zn-cyt *c* into Zn-protoporphyrin and apoprotein. The apoprotein was further decomposed into single amino acid fragments, 1, 2, . . ., 104 residues. The ordinary all-electron calculations were performed for the 104 molecules. Then, all-electron calculations of the 102 tripeptide fragments, 1-3, 2-4, 3-5, . . ., 102-104 were carried out. In this step, the initial electron density was estimated from the corresponding electron density expanded by using the auxiliary functions for each single residue in the results of the previous step. The calculated canonical MOs of the tripeptides were then localized on each atom and the QCLOs for the fragment defined by main-chain or side-chain regions were then obtained. Iterating this type of elongation procedure, we prepared fifteen peptides of the apoprotein: 1-7, 6-14, 13-19, 18-24, 22-30, 29-37, 36-44, 43-51, 50-58, 57-65, 64-72, 71-80, 80-86, 85-95, and 94-104.

The Zn-protoporphyrin part was built up through another elongation pathway. We computed a chromophore model (CM) consisting of Zn-porphine, 5-ethylimidazole for His18 and methyl propyl sulfide for Met80. The geometric data of these elements were derived from the computational structure of Zn-cyt *c* constructed above. We replaced all side chains of protoporphyrin with hydrogen atoms to make Zn-porphine. 5-Ethylimidazole, methyl propyl sulfide, and Zn-porphine were calculated separately, then the model was expanded to the Zn-protoporphyrin complex containing Zn-cyt *c* and its surrounding small peptides, 13-19 and 79-81. All side chains of protoporphyrin were introduced, and Cys14, Cys17, and two vinyl side chains were connected via thioether bonds. Finally we combined the results of the Zn-protoporphyrin complex and the other parts of apoprotein, and carried out the all-electron calculation of Zn-cyt *c*. This calculation includes 1764 atoms, 6590 electrons, and 8786 MOs.

The excited states calculation of chromophore in Zn-cyt *c* was performed by using the TDDFT method[51,52] with the Gaussian 03 (revision B03) program package.[53] The basis sets and the functional are the same as those of the all-electron calculation of Zn-cyt *c*.[45,46,48,49] The model structure was adopted to the CM described above. The symmetry is C_1 and ten excited states of CM were calculated.

Experiments. Chemicals are purchased from Wako, Nacalai and Aldrich, and used without further purification, unless otherwise noted. ω-Sulfhydryl-1-nonanic acid (HOOC-$(CH_2)_{10}$-SH) was purchased from Dojin Co. Native horse heart cyt *c* was purchased from Sigma-Aldrich. Zn-cyt *c* was prepared using Braun's method with slight modifications.[37] Preparation of the gold bead electrode covered by HOOC-$(CH_2)_{10}$-SH (HOOC-SAM) and electrostatic adsorption of Zn-cyt *c* onto HOOC-SAM was carried out by using Tanimura's method.[54]

The optoelectronic measurements were carried out using the system shown in Figure 1. A xenon lamp (Ushio SX-UI150XQ) was used as a light source, and monochromated incident light of which full width at half-maximum was 10 nm was generated by a monochromator (JASCO CT-151T). The incident light was blocked intermittently by a mechanical shutter and focused on the Zn-cyt *c*/HOOC-SAM/Au electrode in a quartz electrochemical cell (10 mM phosphate buffer solution; counter electrode, Pt wire; reference electrode, Ag/AgCl). A potentiostat (Hokuto Denko HA150G) was used to control bias voltage applied to the Zn-cyt *c*/HOOC-SAM/Au electrode against reference electrode, and the time course of the current was recorded.

Results

Excited States of the Chromophore Model (CM). We calculated the ten excited states of the six-coordinated Zn-porphine complex. The CM structure is shown in Figure 2, and detailed information on the excited states is given in Table 2. In an ordinary case, first and second excited states would be assigned to the transition responsible for absorption in the Q-band[38,55,56] However, the oscillator strengths (OS) for these states having a Por(σ) $\rightarrow$ Por(π^*) nature (1^1A and 2^1A) appeared to be relatively small states. Thus, these two states could not be assigned to the Q-band. On the other hand, 3^1A and 4^1A states have a Por(π) + Zn$-$S(π) $\rightarrow$ Por(π^*) nature and the OSs (2.5×10^{-3} and 1.5×10^{-3}, respectively) are relatively larger than those of 1^1A and 2^1A states. Therefore, we assigned them to the Q-band, though the energies calculated, 1.47 and 1.59 eV, were somewhat lower than the experimental value, around 2.2 eV.[37]

5^1A and 6^1A states also have the same nature as 3^1A and 4^1A states and the OSs (1.1×10^{-2} and 9.3×10^{-3}, respectively) are about ten times larger than those of 3^1A and 4^1A states, so we assigned these states to the Soret band.

In this way, the four MOs responsible for excitation by UV–vis light (Gouterman's 4-orbitals) of CM were assigned to MOs 144, 145, 147 (LUMO), and 148, as shown in Figure 3.[38] It appears that MOs 144 and 145 have a porphyrin π with Zn$-$S π-bonding nature, which is consistent with the fact that the Zn$-$S (Met80) bond dissociates upon photoexcitation in Zn-cyt *c*.[29]

All-Electron Wave Functions of Zn-cyt *c* (Ground State). The Khon$-$Sham orbital energy and character of Zn-cyt *c* are shown in Table 3 and the MOs with a porphyrin π-nature are depicted in Figure 4. The porphyrin π-type, occupied MOs 3268, 3271, 3272, and 3287 have a more stable energy away from the HOMO–LUMO region. Natures of occupied MOs in the higher energy region are essentially those of the corresponding amino acid derivatives. It should be noted that MOs 3268 and 3272 possess Zn$-$S (Met80) π-bonding nature, as well. Since the nature of these MOs is the same as those of 4-orbitals for CM (MOs 144 and 145), as is clearly seen in Figure 3 (c$-$f) and Figure 4 (a,b), we assigned MOs 3268 and 3272 to the occupied

(47) Gill, P. M. W.; Johnson, B. G.; Pople, J. A. *Chem. Phys. Lett.* **1993**, *209*, 506–512.
(48) Godbout, N.; Salahub, D. R.; Andzelm, J.; Wimmer, E. *Can. J. Chem.-Rev. Can. Chim.* **1992**, *70*, 560–571.
(49) Andzelm, J.; Radzio, E.; Salahub, D. R. *J. Comput. Chem.* **1985**, *6*, 520–532.
(50) Kashiwagi, H.; Iwai, H.; Tokieda, K.; Era, M.; Sumita, T.; Yoshihiro, T.; Sato, F. *Mol. Phys.* **2003**, *101*, 81–86.
(51) Bauernschmitt, R.; Ahlrichs, R. *Chem. Phys. Lett.* **1996**, *256*, 454–464.
(52) Stratmann, R. E.; Scuseria, G. E.; Frisch, M. J. *J. Chem. Phys.* **1998**, *109*, 8218–8224.
(53) Frisch, M. J.; et al. *Gaussian 03*, revision B.03; Gaussian, Inc.: Wallingford, CT, 2004.
(54) Tanimura, R.; Hill, M. G.; Margoliash, E.; Niki, K.; Ohno, H.; Gray, H. B. *Electrochem. Solid State Lett.* **2002**, *5*, E67–E70.
(55) Nakatsuji, H.; Hasegawa, J.; Hada, M. *J. Chem. Phys.* **1996**, *104*, 2321–2329.
(56) Tokita, Y.; Hasegawa, J.; Nakatsuji, H. *J. Phys. Chem. A* **1998**, *102*, 1843–1849.

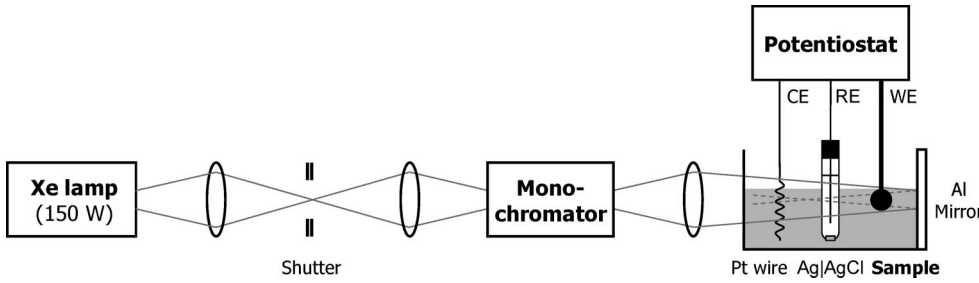

Figure 1. Photoelectrochemical measurement system. CE is a Pt wire counter electrode, RE is an Ag/AgCl (saturated KCl) reference electrode, and WE is a Zn-cyt *c*/HOOC-SAM/Au working electrode.

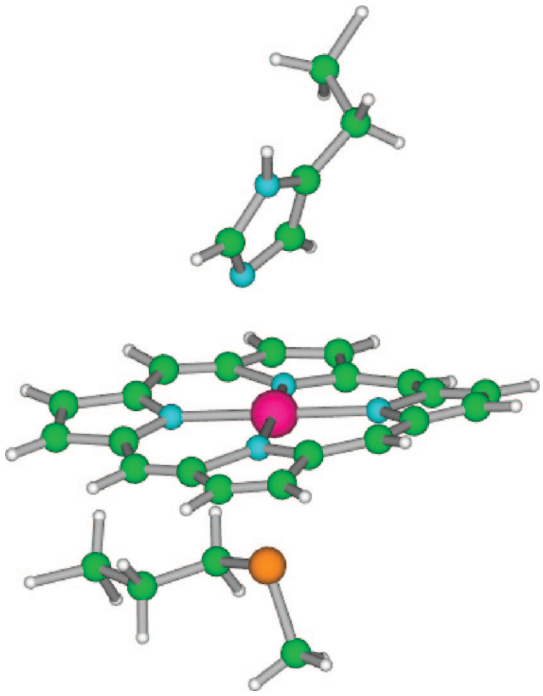

Figure 2. Structure of chromophore model complex. Magenta, orange, light blue, light green, and white are zinc, sulfur, nitrogen, carbon, and hydrogen, respectively.

Gouterman's 4-orbitals of Zn-cyt *c*. MO 3271 has nature of the asparagine-54 (Asn54) derivative, whose shape is similar to that of MO 3272, though the main nature is not a porphyrin π-type but an Asn54.

The porphyrin π^*-type unoccupied orbitals 3297 and 3299 are in the lower energy region. Since shapes of these two MOs are almost the same as those of the 4-orbitals for CM (MOs 147 and 148), as shown in Figure 3a,b and Figure 4c,d, we assigned these MOs to the unoccupied Gouterman's 4-orbitals of Zn-cyt *c*.

ET Analysis by Using Fermi's Golden Rule.[39,40] Since we have obtained the precise all-electron wave function of Zn-cyt *c* and have assigned the MOs related to the excited states, we can calculate the ET rate-constant from MO to MO using Fermi's golden rule,

$$k_{i\to f} = \frac{2\pi}{\hbar}|\langle f|H'|i\rangle|^2\rho \qquad (2)$$

where H' is perturbing Hamiltonian, $|i\rangle$ and $|f\rangle$ are an initial and final eigenstates, respectively, ρ is the density of final state, and $\langle f|H'|i\rangle$ is the matrix element of the perturbation (for example time-dependent), H', between initial and final states. We can divide $\langle f|H'|i\rangle$ into two parts: one is a Franck–Condon factor and another is the electronic coupling matrix element. In the present case, since we have canonical MOs, which means the overlap matrixes between MOs are zero, H' can be approximated to H that is time independent Hamiltonian.[15] Furthermore, ρ can be described as delta-function of the energy difference between final and initial states.

$$k_{i\to f} = \frac{2\pi}{\hbar}(\mathrm{FC})|\langle f|H_{\mathrm{el}}|i\rangle|^2\delta(E_{\mathrm{fi}}) \qquad (3)$$

where (FC) is a Franck–Condon factor, H_{el} is a time-independent electron Hamiltonian, $\langle f|H_{\mathrm{el}}|i\rangle$ is the electronic coupling matrix between initial and final states, and E_{fi} is the energy difference between final and initial states. We adopted one-electron model in the present analysis,[15] so the electronic coupling matrix elements can be described as

$$\langle f|H_{\mathrm{el}}|i\rangle \approx \langle \varphi_f|H_{\mathrm{el}}|\varphi_i\rangle = H_{\mathrm{fi}} \qquad (4)$$

where φ_f and φ_i are effective final and initial molecular orbitals, respectively, and (FC) approximates to 1, assuming that (FC) is constant. Thus, the ET rate constant is described as

$$k_{i\to f} = \frac{2\pi}{\hbar}H_{\mathrm{fi}}\delta(E_{\mathrm{fi}}) \qquad (5)$$

We analyzed the electronic coupling matrix elements of Gouterman's 4-orbitals of Zn-cyt *c*. These matrix elements corresponding to F' matrix of Hartree–Fock theory were calculated from unitary conversion of the final Fock matrix of the Kohn–Sham−Roothaan equation.[57] Figure 5 shows the H_{fi} for MOs 3268, 3272, 3297, and 3299, respectively. ET rate constants were estimated from eq 5 as shown in Figure 6. Clearly, the rate constant between MOs 3272 and 3271 was extremely large (1.5×10^{11} sec^{-1}), compared with the others as shown in Figure 6a. MO3271 is localized on the outermost amino acid residue, Asn54, implying that the ET pathway is solely defined by MOs 3272 and 3271. Similarly, the rate constant between MOs 3268 and 3270 localized on the outermost amino acid residue, Lys 7 is also very large, 2.0×10^{10} sec^{-1} (Figure 6b). On the other hand, the rate constants of unoccupied 4-orbitals between MOs 3297 and 3296 localized on outermost amino acid residue Glu62 and between MOs 3299 and 3298 localized on outermost amino acid residue Asp93 are 5.5×10^8 sec^{-1} and 2.8×10^8 sec^{-1}, respectively, which are relatively smaller than those of the occupied 4-orbitals (Figure 6c,d). From these analyses, the long-distance ET in photoexcited Zn-cyt *c* could be governed by the occupied 4-orbitals, MOs 3268 and 3272 having a

(57) Parr, R. G.; Yang, W. *Density-Functional Theory of Atoms and Molecules*; Springer-Verlag: Tokyo, 1996.

Table 2. Excited States of Zn-Porphine Complex (CM)

state	main configurations |c| > 0.25	nature[b]	excitation energy (eV)	oscillator strength	experiment[a](eV)
1^1A	0.69 (146→147)	Por(σ)→Por(π^*)	1.35	2.0×10^{-4}	
2^1A	0.69 (146→148)	Por(σ)→Por(π^*)	1.45	1.0×10^{-4}	
3^1A	0.64 (145→147) +0.27 (144→147)	Por(π) + Zn−S(π) →Por(π^*)	1.47	2.5×10^{-3}	2.13 (Q)
4^1A	0.58 (145→148) +0.39 (144→148)	Por(π) + Zn−S(π) →Por(π^*)	1.59	1.5×10^{-3}	2.27 (Q)
5^1A	0.60 (144→147)	Por(π) + Zn−S(π) →Por(π^*)	1.80	1.1×10^{-2}	2.94 (Soret)
6^1A	0.50 (144→148) −0.29 (143→147) −0.26 (145→148)	Por(π) + Zn−S(π) →Por(π^*)	2.09	9.3×10^{-3}	2.94 (Soret)
7^1A	0.59 (141→147) +0.30 (142→147)	Por(π) + Im(π) →Por(π^*)	2.45	3.0×10^{-4}	
8^1A	0.43 (142→147) −0.38 (141→147) −0.27 (143→148)	Por(π) + Im(π) →Por(π^*)	2.48	1.3×10^{-3}	
9^1A	0.56 (142→148) +0.26 (141→148)	Por(π) + Im(π) →Por(π^*)	2.50	2.8×10^{-3}	
10^1A	−0.65 (141→148)	Por(π) + Im(π) →Por(π^*)	2.56	6.0×10^{-4}	

[a] Reference 37. [b] Por(σ) and Por(π) denote the porphyrin σ and π MOs, respectively. Zn−S(π) is the Zn−S π-bonding nature. Im(π) denotes the imidazole π MO.

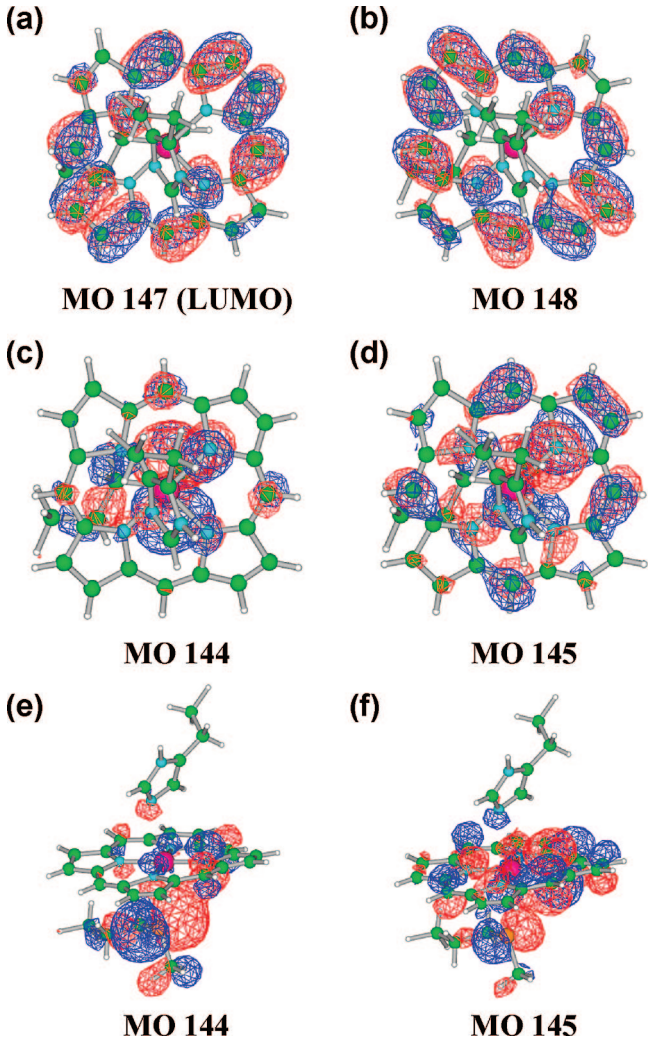

Figure 3. Gouterman's 4-orbitals for chromophore model: (a) top view of MO 147 (LUMO), (b) top view of MO 148, (c) top view of MO 144, (d) top view of MO 145, (e) side view of MO 144, and (f) side view of MO 145.

Por(π) + Zn−S(π) nature, and the MOs 3270 and 3271 localized on the outermost amino acid residues.

Table 3. Khon−Sham Orbital Energies and Nature of Zn-cyt *c*

MOs	energy (eV)	nature[a]
3268	−6.46	Por(π), Zn−S(π)
3269	−6.45	Glu69
3270	−6.44	Lys7
3271	−6.42	Asn54, Por(π)
3272	−6.42	Por(π), Zn−S(π),Asn54
3273	−6.39	Ala83
3274	−6.37	Gly23, His33
3275	−6.37	Gly37, Arg38
3276	−6.36	Gly23, His33
3277	−6.30	Gln12
3278	−6.23	Arg38
3279	−6.19	Gln12
3280	−6.16	Arg38
3281	−6.16	His33
3282	−6.08	Ala83
3283	−6.03	Por(σ)
3284	−5.97	Gln12
3285	−5.93	Glu69
3286	−5.92	Gly37
3287	−5.92	Por(π)
3288	−5.86	Gln16
3289	−5.76	Gln16
3290	−5.72	Thr58
3291	−5.63	Cys17
3292	−5.60	Ala15
3293	−5.58	Lys100
3294	−5.45	Glu69
3295 (HOMO)	−5.06	Gln16
3296 (LUMO)	−4.46	Glu62, Por(π^*)
3297	−4.45	Por(π^*)
3298	−4.40	Asp93, Por(π^*)
3299	−4.29	Por(π^*)

[a] See the footnotes of Table 2. The abbreviations of amino acids are as follows: Glu69, glutamic acid No. 69 from N-terminal; Lys7, lysine No. 7; Asn54, asparagine No. 54; Ala83, alanine No. 83; Gly23, glycine No. 23; His33, histidine No. 33; Gly37, glycine No. 37; Arg38, arginine No. 38; Gln12, glutamine No. 12; Gln16, glutamine No. 16; Thr58, threonine No. 58; Cys17, cysteine No. 17; Ala15, alanine No. 15; Lys100, lysine No. 100; Glu62, glutamic acid No. 62; Asp93, aspartic acid No. 93. The nature arranges in order of weight.

Photocurrents of Zn-cyt *c*/HOOC-SAM/Gold Electrode System. The orientation of cyt *c* on a HOOC-SAM/Au electrode and the electron pathway between the heme and electrode have

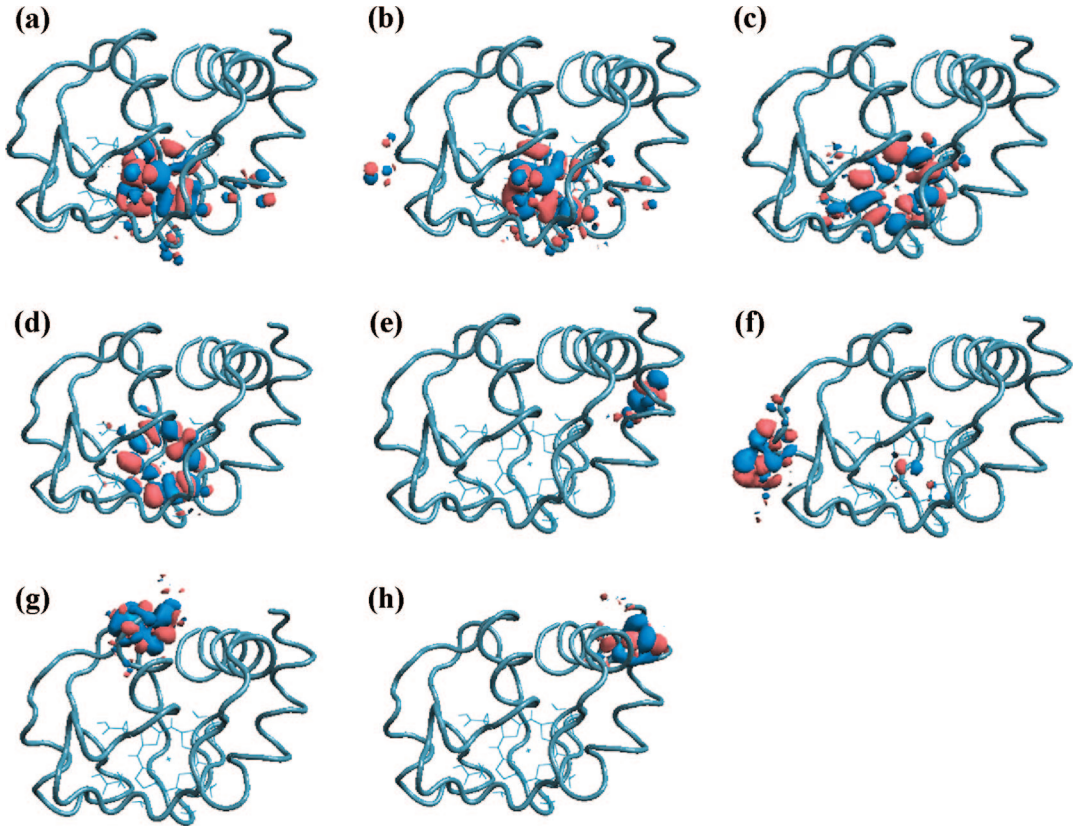

Figure 4. Main MOs related to the photoexcitation and ET of Zn-cyt *c*: (a) MO 3268, (b) MO 3272, (c) MO 3297, (d) MO 3299, (e) MO 3270, (f) MO 3271, (g) MO 3296 (LUMO), (h) MO 3298. Structures a−d are Gouterman's 4-orbitals of Zn-cyt *c*. Sturctures e and f are MOs coupled strongly with structures a−b, repsectively. The isosurface values are ±0.01.

been previously discussed by Xu et al.[58] and Zhou et al.[59] They demonstrated that the heme edge exposed to the electrode surface renders facile ET. Since the molecular structure of Zn-cyt *c* is proven to be almost identical with that of native cyt *c* by NMR, it is reasonable to assume that the orientation of Zn-cyt *c* on the HOOC-SAM electrode is essentially the same as that of native cyt *c* that the lysine patch electrostatically interacts with anionic charge of the SAM surface (Scheme 1).[41,60,61] Therefore, ET can occur between the zinc-protoporphyrin in Zn-cyt *c* and the electrode surface as it does in native cyt *c*. By contrast, the protein scaffold should serve as the route for electron migration between the zinc- protoporphyrin and redox agents in solution.

We measured the time-resolved photocurrents by irradiating monochromic light at 420 nm that corresponds to the absorption maximum in the Soret band of Zn-cyt *c*. Figure 7a shows the rise and fall of the anodic photocurrents in response to the switching on and off of the light irradiation under the bias potential of +503 mV (vs Ag/AgCl). Similarly, cathodic photocurrents are observed when applying a bias potential of −77 mV (Figure 7b). Figure 8 shows action spectrum of anodic photocurrent observed for the Zn-cyt *c*/HOOC-SAM/Au working electrode at an applied potential of 503 mV with a platinum counter electrode. The action spectrum can be superimposed on the UV–vis spectrum of Zn-cyt *c*, indicating that the photocurrent in the UV–vis region originated from its absorption and that Zn-cyt *c* fixed on the HOOC-SAM electrode retains its original coordination structure.

Figure 9 shows dependence of the photocurrents upon the bias potentials applied for the electrode. Both anodic and cathodic photocurrents are virtually on a straight line in the range of the potential employed in this study with the transverse intercept at 79 mV. This photocurrent behavior indicates Zn-cyt *c* is photoconductive. In other words, the photoconductor system based on the single-protein, Zn-cyt *c*, was constructed for the first time.

Discussion

To get a clue to understanding the long-range ET in protein, we analyzed an intramolecular ET mechanism in protein on the basis of the precise all-electron wave function of the photoexcited Zn-cyt *c* calculated with DFT method. We have found that MOs around HOMO–LUMO region have a nature localized either on the amino acid residues or on chromophore. Since we can directly estimate H_{fi} and E_{fi} from DFT calculation, the rate constants of long-distance ET could be also estimated with Fermi's golden rule using two-states and one-electron models. The results suggest that there are specific pathways of ET through the occupied MOs of Zn-cyt *c*; between MOs 3272 (Por(π) + Zn−S(π)) and 3271 (Asn54), and between MOs 3268 (Por(π) + Zn−S(π)) and 3270 (Lys7) and the long-distance ET can be described as the superexchange scheme.[15,62] Although

(58) Xu, J.; Bowden, E. F. *J. Am. Chem. Soc.* **2006**, *128*, 6813–22.
(59) Zhou, J.; Zheng, J.; Jiang, S. Y. *J. Phys. Chem. B* **2004**, *108*, 17418–17424.
(60) Ye, S. Y.; Shen, C. Y.; Cotton, T. M.; Kostic, N. M. *J. Inorg. Biochem.* **1997**, *65*, 219–226.
(61) Anni, H.; Vanderkooi, J. M.; Mayne, L. *Biochemistry* **1995**, *34*, 5744–53.
(62) McConnell, H. M. *J. Chem. Phys.* **1961**, *35*, 508–515.

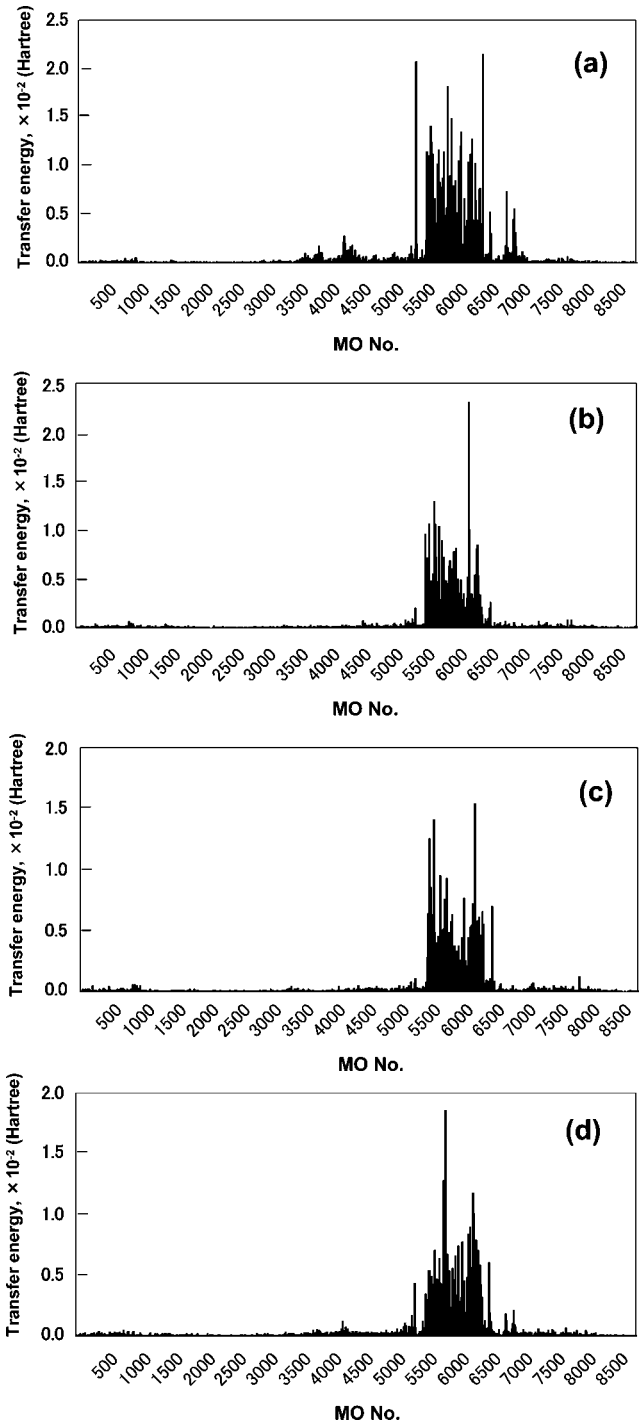

Figure 5. Electron transfer energies (H_{fi}) coupled with Gouterman's 4-orbitals of Zn-cyt *c*: (a) MO 3268, (b) MO 3272, (c) MO 3297, (d) MO 3299.

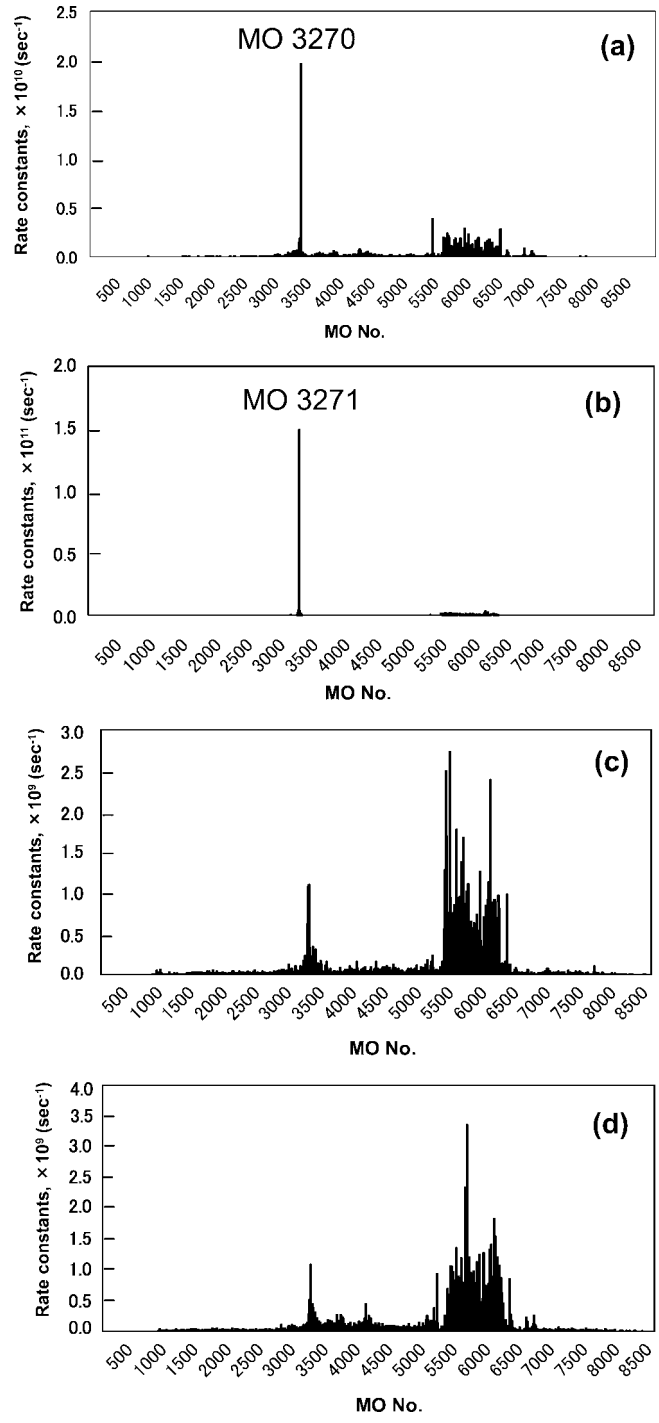

Figure 6. Electron transfer rate constants coupled with Gouterman's 4-orbitals of Zn-cyt *c*: (a) MO 3268, (b) MO 3272, (c) MO 3297, (d) MO 3299.

both rate constants are significantly larger than the others, the two factors H_{fi} and E_{fi} contribute differently in determining the rates. In the case of MO 3272 coupled with MO 3271 ($k_{i\rightarrow f} = 1.5 \times 10^{11}$ sec^{-1}), H_{fi} of 6.1×10^{-2} eV is not significantly larger than those of MOs around MO 3272 (1.3×10^{-4} to ca. 2.7×10^{-1} eV) and E_{fi} of 9.2×10^{-5} eV is extremely smaller than the other E_{fi} values, hence the rate constant is governed by the delta function, $\delta(E_{fi})$ in eq 5. On the other hand, in the case of MO 3268 coupled with MO 3270 ($k_{i\rightarrow f} = 2.0 \times 10^{10}$ sec^{-1}), H_{fi} of 3.5×10^{-1} eV is relatively larger than those of MOs around MO 3268 and E_{fi}, 2.3×10^{-2} eV, is relatively smaller than others, hence the rate constant is governed both by H_{fi} and by $\delta(E_{fi})$.

In the case of the unoccupied MOs, MO 3297 coupled with MO 3296 ($k_{i\rightarrow f} = 5.5 \times 10^{8}$ sec^{-1}) and MO 3299 coupled with MO 3298 ($k_{i\rightarrow f} = 2.8 \times 10^{8}$ sec^{-1}) are significantly smaller than those of the occupied MOs, indicating that the ET through the unoccupied MOs is not dominant in the photoexcited Zn-cyt *c* and the excited electron has a long lifetime. Actually, our calculated rate constants of fluorescence decay (Por(π^*)→Por(π)) are 2.9×10^{8} sec^{-1} (MO 3299 → MO 3272), 2.0×10^{8} sec^{-1}

Scheme 1. The Orientation of Zn-cyt *c* Immobilized on HOOC-SAM Fabricated on an Au Electrode.

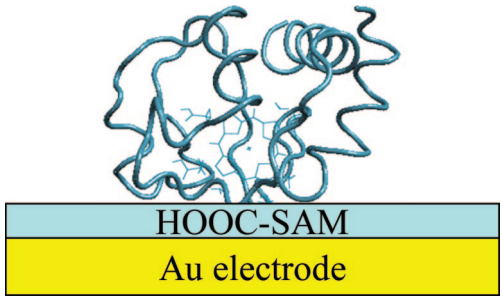

(MO 3299 → MO 3268), 1.0×10^8 sec^{-1} (MO 3297 → MO 3272), and 2.5×10^8 sec^{-1} (MO 3297 → MO 3268) are very close to that of the singlet excited-state on Zn-cyt *c* ($<5.0 \times 10^8$ sec^{-1})[63] and these values are also close to the calculated long-distance ET rate constants of the unoccupied 4-orbitals (see the ET Analysis by Using Fermi's Golden Rule section).

From these analyses based on two-state and one-electron models, we found that the major factor of ET in the photoexcited Zn-cyt *c* could be "hole transfer (HT)" through two-states coupling between occupied MOs. This description may comprehend both Dutton's model and Gray's model. According to the H_{fi} analyses, the H_{fi} values around the 4-orbitals region are almost homogeneous and their influences on ET rate constants should be relatively small. Hence, if the $\delta(E_{fi})$ effect is small, the ET rate will be well-described with Dutton's model where a mass of peptides can be treated as a continuous medium.[6,7] On the other hand, the Gray model is rather preferable when the effect of $\delta(E_{fi})$ is not negligible.[3–5]

How can protein control H_{fi} and $\delta(E_{fi})$? In the present calculation, the extremely large HT rate of the photoexcited Zn-cyt *c* is controlled not only by the larger H_{fi}, but also by the smaller E_{fi} values. Particularly in Zn-cyt *c,* the small E_{fi} value is important for the extremely high rate constants of HT. In general, energetic states of Gouterman's 4-orbitals of metalloporphyrins, however, are unstable compared to those of MOs localized on amino acid residues, because the two occupied 4-orbitals have a porphyrin-π nature of a long conjugated system. So, it is suggested that Zn-cyt *c* (or cyt *c*) has a particular molecular structure to realize a small E_{fi}. The Zn-protoporphyrin in Zn-cyt *c* has two axial ligands, His17 and Met80. Met80 with sulfur ligation is expected to play an important role in the stabilization of the occupied 4-orbitals as is proposed for cytochrome P-450 having an axial cystein ligand with sulfur ligation.[64–66] In CM calculation the energies of porphyrin π orbitals including a Zn−S π-bonding nature (MOs 144 and 145) are also more stable than those of the porphyrin σ orbital, MO 146 as shown in Table 2. Consequently, the energy control of the porphyrin π MOs by ligation of axial ligands is essential to the intramolecular HT in photoexcited Zn-cyt *c*.

To examine proposed ET (or HT) mechanism of photoexcited Zn-cyt *c*, we have prepared a Zn-cyt *c*/HOOC-SAM/Au electrode and measured the photocurrents under irradiation of UV–vis light. On the analogy with native cyt *c* on the modified electrode, Zn-protoporphyrin site (photoactive site) is

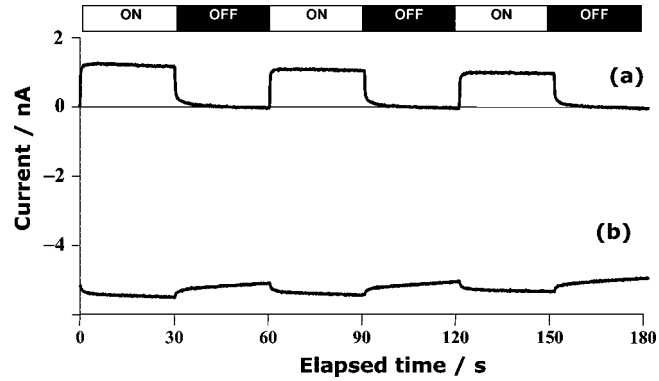

Figure 7. Photo currents of the Zn-Cyt *c*/HOOC-SAM/Au electrode to illumination at 420 nm in N_2-saturated 10 mM phosphate buffer (pH 7.0). Applied bias potentials are (a) +503 mV (vs Ag/AgCl) and (b) –77 mV.

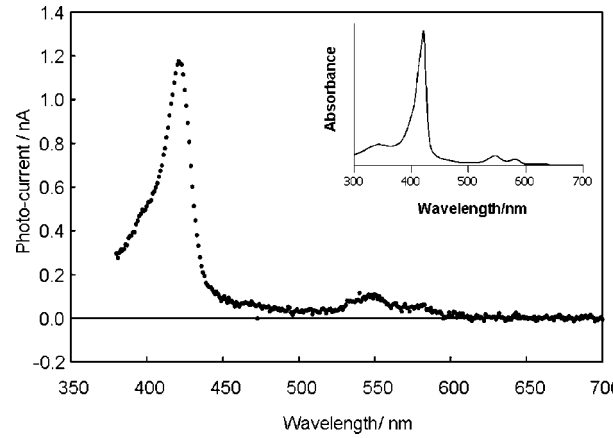

Figure 8. Plots of the photocurrents of the Zn-cyt *c*/HOOC-SAM/Au electrode incorporated in a three electrode photochemical cell with 2.5 mM $K_4[Fe(II)(CN)_6]$ in an N_2-saturated 10 mM phosphate buffer (pH 7.0). The potential applied for the Zn-cyt *c*/HOOC-SAM/Au electrode was held at +503 mV (vs Ag/AgCl). The inset depicts a UV–vis absorption spectrum of Zn-cyt *c* in the buffer solution. The resolution of the action spectrum is 1 nm.

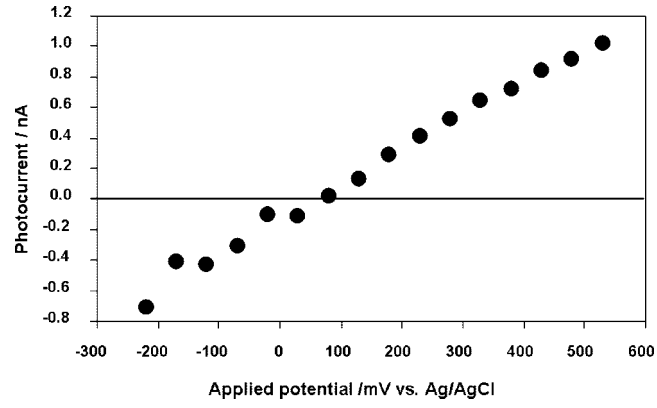

Figure 9. Dependence of photocurrent on bias potential applied for the Zn-cyt *c*/HOOC-SAM/Au electrode. Photocurrents of each plot are observed under illumination at 420 nm in N_2-saturated 10 mM phosphate buffer (pH 7.0).

expected to be close to the SAM surface, whereas Asn54 and Lys7 are exposed to the solution. This electrode is thus suitable to examine the intramolecular ET (or HT) in the photoexcited Zn-cyt *c*; a photoconductive character should be observed, if the HT mechanism based on the present DFT calculations is correct. As shown in Figure 9, the photocurrent–voltage response

(63) Sudha, B. P.; Dixit, N.; Moy, V. T.; Vanderkooi, J. M. *Biochemistry* **1984**, *23*, 2103–2107.
(64) Miyahara, T.; Tokita, Y.; Nakatsuji, H. *J. Phys. Chem. B* **2001**, *105*, 7341–7352.
(65) Loew, G. H.; Rohmer, M.-M. *J. Am. Chem. Soc.* **1980**, *102*, 3655–3657.

of Zn-cyt *c*/HOOC-SAM/Au system is linear-dependent and bidirectional, which strongly supports the proposed HT mechanism. Furthermore, the photocurrent action spectrum is almost the same as the UV–vis absorption spectrum of Zn-cyt *c*, indicating that this photocurrent is derived from migration of the hole on the occupied MOs. This is in good contrast to the Zn cyt *c*/metal oxide semiconductor system,[67,68] where the Soret/Q-band ratio in the observed action spectrum is different from that in the absorption spectrum of Zn-cyt *c* because the photocurrent is derived from migration of the excited electron.

Conclusions

In this paper, we have successfully calculated an all-electron wave function for the ground states of Zn-cyt *c* protein on the basis of the DFT method, and assigned Gouterman's 4-orbitals by using TDDFT for CM of Zn-cyt *c* center. In an attempt to understand the mechanism of the photoinduced ET in Zn-cyt *c*, we have analyzed the intramolecular ET rate between each of the Gouterman's 4-orbitals and the rest of the MOs by applying Fermi's golden rule. The mechanistic finding of this analysis is twofold. First, the two pathways of photoinduced ET have been assigned: we found that the rate of ET is predominantly high between each of the two occupied Gouterman's 4-orbitals and particular amino acid residues on the protein surface, Asn54 and Lys7, respectively. On the other hand, the rates of ET from the two unoccupied Gouterman's 4-orbitals are less significant. Thus the intramolecular photoinduced ET in Zn-cyt *c* would be driven by hole transfer through occupied MOs. Second, in those electron transfer process, electronic coupling elements (H_{fi}) and/or energy differnce between the two MOs (E_{fi}) determines the rate of electron transfer. It is implicated that this type of analysis may comprehensively describe the two proposed mechanisms for the electron transfer in protein: Dutton's model in which ET rate is dependent upon donor–acceptor distance, and Gray's model in which it is rather dependent upon number of chemical bonds connecting donor and acceptor.

Futhermore, the ET process through occupied MOs has been demonstrated by photochemical studies with Zn-cyt *c* immobilized on a gold electrode by SAM method: We have found that the action spectrum of the photocurrent is superimposable with the electronic spectrum of Zn-cyt *c* and that the photocurrent is linearly dependent upon bias voltage on the gold electrode, both of which are well-consistent with the reaction mechanism indicated in the analysis based on the calculation.

It is shown that determination of precise electronic states of a protein can be useful in studies on ET chemistry in the protein. Further experimental studies focused on roles of the amino acid residues that would be involved in the ET in cytochrome *c* are underway.

Acknowledgment. We thank S. Koike (AdvanceSoft Corporation) for detailed discussion about proteinDF. Y.T., J.S., and Y.G. thank Daisuke Hobara (SONY) and Keiko Yokoyama (California Institute of Technology) for their useful suggestions in preparation of Au electrodes.

Supporting Information Available: Complete ref 53, Cartesian coordinate of Zn-cyt *c* used by the all-electron DFT calculation, and Cartesian coordinate of CM. This material is available free of charge via the Internet at http://pubs.acs.org.

JA711324T

(66) Luke, B. T.; Collins, J. R.; Loew, G. H.; McLean, A. D. *J. Am. Chem. Soc.* **1990**, *112*, 8686–8691.
(67) Guo, L. H.; Mukamel, S.; McLendon, G. *J. Am. Chem. Soc.* **1995**, *117*, 546–547.
(68) Topoglidis, E.; Campbell, C. J.; Palomares, E.; Durrant, J. R. *Chem. Commun.* **2002**, 1518–1519.